# Improvement of Sandy Soil with Cylindrical Cavity by Using Geogrids

**Laith Jawad Aziz**
*Civil Dep./ College of Engineering/ Kufa University*
laith.aljarrah@uokufa.edu.iq

## Abstract

This study is focuses with the possibility of using Tanser SS2 geogrid as a reinforcement material to increase the bearing capacity and reduce settlement under strip foundation located on sandy soil with cylindrical cavity. Forty five laboratory model tests were conducted using a steel box with 1250 mm in length, 800 mm in depth and 250 mm in width. Increment loads were applied on strip footing with 100 mm in width and 250 mm in length. Since the length of the model foundation was approximately the same as the width of the test box and length of the cavity, it can be assumed that an approximate plane strain condition exist during the tests. For each model, the relationship between the applied pressure and the corresponding settlement was detected.

From the results of a series of laboratory tests, it was found that the bearing capacity ratio (BCR) of the soil increases with increasing in width of geogrid, (b/d) specially when the cavity center coincides with the centerline of the strip footing (X/d=0). The effect of geogrid width will reduce with moving the cavity away from the strip footing. When the width of the geogrid layer was high (b/d), the maximum increase in bearing capacity ratio can be noticed at high depth of geogrid layer (h/d=3), and this bearing capacity ratio becomes very low at small geogrid width for same value of (h/d=3).

At zero lateral distance ratio (X/d) and two layer reinforced, the higher generated bearing capacity are noted when the vertical distance between two layer geogrid is (S/d=1, i.e optimum value), but at (S/d=0.5), the values of footing resistance are lowest. The effects of number of layer (N) on the bearing capacity of strip footing are very small at low value of geogrid width. At geogrid width (b/d >1), the case of geogrid (N=3, i.e optimum value) record the highest values of the bearing capacity ratio. The location of peak strain readings of the geogrid surface is depends upon the cavity position. As the geogrid layers were near to the base of the footing, the values of reinforcement strains were increased.

**Keywords: Sandy Soil, Cavity, Geogrid Reinforced, Strip Footing, Soil Improvement**

## الخلاصة:

هذا البحث يركز على إمكانية استخدام التسليح Geogrid Tanser SS2 لزيادة قابلية تحمل التربة و لتقليل الهبوط أسفل أساس شريطي موجود فوق تربة رملية حاوية على فجوات. خمسة و أربعون موديل مختبري تم انجازه باستخدام حاوية حديدية ذات طول ( ١٢٥٠ ملم وعمق ٨٠٠ ملم و عرض ٢٥٠ ملم). تحميل تراكمي يسلط على أساس شريطي ذي عرض( ١٠٠ ملم و طول ٢٥٠ ملم). الطول لموديل الأساس يكون مساوي إلى عرض الحاوية الحديدية و بدوره يكون مساوي إلى طول الفجوة و في هذه الحالة يمكن فرض الحالة كتشوه سطحي تقريباً و لجميع الفحوصات. لكل فحص العلاقة بين الإجهاد المسلط و النزول المناظر له تكون مقاسة.

من النتائج لمجموعة الفحوصات المختبرية يمكن أن نجد بان نسبة قابلية التحمل للتربة تزداد مع زيادة عرض الجيوكرد و خصوصاً عندما مركز الفجوة ينطبق مع مركز الأساس الشريطي. التأثير لعرض الجيوكرد سوف يقل مع ازاحة الفجوة بعيدا عن الأساس الشريطي. عندما يكون عرض طبقة الجيوكرد كبير، قيمة نسبة قابلية التحمل تكون قصوى و يمكن أن نلحظها عند نسبة عمق كبيرة مساوية إلى ( ٣ ) ، و قيمة نسبة قابلية التحمل تصبح ذات قيمة واطئة جداً عندما يكون عرض الجيوكرد صغير عند نفس قيمة نسبة العمق ( ٣ ).

عندما تقع الفجوة أسفل مركز الأساس و عندما يتم تسليح التربة بطبقتين من الجيوكرد، أعلى نسبة لقابلية تحمل التربة يمكن تسجيلها عندما تكون نسبة البعد العمودي بين الطبقتين مساوي إلى (١)، و لكن عندما تكون نسبة البعد العمودي بين الطبقتين مساوي (٠,٥)، القيم لمقاومة الأساس تكون الأصغر. التأثيرات لعدد الطبقات على قابلية التحمل لأساس مستمر تكون صغيرة جداً عند قيم واطئة لعرض الجيوكرد. و عندما تكون قيم عرض الجيوكرد اكبر من واحد، فان الموديل الحاوي على ثلاث طبقات سيسجل أعلى قيم لنسبة قابلية التحمل. الموقع لأقصى انفعال يتولد على سطح الجيوكرد يعتمد على موقع الفجوة الأفقي. كلما طبقات الجيوكرد تكون قريبة من قاعدة الأساس الحصيري، القيم لانفعالات التسليح تزداد.

**كلمات الاستدلال:** التربة الرملية، الفجوة، التسليح بالجيوكرد، الاساس الشريطي، تسليح التربة

**List of Symbols**

B/d : h of the footing to diameter of the cavity.
BCR : ıltimate bearing capacity of soil with geogrid reinforcement to the ultimate bearing capacity of soil without geogrid reinforcement.
b/d : Width of geogrid layer to diameter of the cavity.
D/d : Depth to diameter of the cavity.
$D_f$/d : Depth of the strip footing below ground surface level to the diameter of the cavity .
h/d : Depth of first geogrid layer to diameter of the cavity.
q : Ultimate bearing capacity of sandy soil with cavity when the soil is reinforced.
$q_n$ : Ultimate bearing capacity of sandy soil with cavity when the soil is not reinforced.
S/d : The vertical distance between geogrid layers to diameter of the cavity.
X/d : The offset distance from the footing centerline to the centerline of the cavity.
δ/d : Average settlement along the centerline of strip footing to diameter of the cavity.

**1-Introduction**

The purpose of any soil improvement study is to generally increase soil unit weight, increase soil allowable bearing capacity, reduce settlement under foundation loads to the allowable limits.**[ Al-Fares, 2008]**.

The use of geogrid layers could be particularly convenient when the mechanical characteristics of the soil beneath a foundation would suggest the designer in adopting an alternative solution, e.g. a deep foundation. Over the last decade, the use of geogrids for soil reinforcement has increased greatly, primarily because geogrids are dimensionally stable and combine features such as high tensile modulous (low strain at high load), open grid structure, positive shear connection characteristics,light weight, and long service life. The open grid structure provides enhanced soil-reinforcement interaction.**[Patra, 2005]**.

When designing structures that will impose a significant load over a large area, such as buildings, tanks, walls, slopes or embankments, geotechnical engineers must address the following situations, especially when dealing with weak foundation soils: bearing capacity failures, in tolerable total and differential settlements, large lateral pressures and movement, and slope instability. **[Al-Sinaidi and Ali, 2006 ]**. For weak foundation soils such as soil with cavities, the construction of reinforced soil foundations must be used to support these structures. During excavation of Al-Najaf soil site to take many samples, a network of interconnect cavities were found to exist at depths ranging from (0.1) to (2) meters. These cavities formed due to the ground water movement towards the Al-Najaf sea. This movements of groundwater have caused dissolution of gypsum in Al-Najaf city soil.

**2-Review of Literature**

A few number of the published studies on the stability of strip footing located above sandy soil with cavity when the soil reinforced. Theoretical analysis of the soil reinforcement, which contained cavities dated back to 1994 when Gabr and Hunter investigated the magnitude of tensile strains imposed on landfill liners due to the formation of subsurface cavities by using finite element analyses. The study incorporated the significance of using geogrids to reduce the magnitude of strains and possibly the potential for collapse of landfill liners. Variations of key parameters included depth of overburden (D) and diameter of the cavity (d). Results indicated that, incorporation of geogrid reinforcement reduced the magnitude of tensile strains. The tensile force in the geogrid was dependent upon the size of the cavity, the depth of the overburden, and the applied pressure.

In recently, 2008, Ghazavi and Soltanpour investigated the influence of type of footing on the bearing capacity of soil reinforced with Geotextile layer when this shallow foundations constructed above underground cavities at a specific value of cavity location, number of Geotextile layer, geotextile width, depth of the first layer of geotextile, and the vertical distance between the geotextile layers. Accordingly, FLAC 3D software (version 3) was used to simulate the 'cavity-reinforcement-footing' system. In the analysis, value of 5 kN/m$^2$ was assumed for the soil cohesion. The soil friction angle was assumed to be 35$^o$. A comparison was made with the case where no reinforcement layer was used. The results have shown that the bearing capacity ratios (BCR) are 1.13, 1.01, and 1.22 for strip, square, and circular foundations respectively. It is generally found that the reinforcement of the soil above the cavity crest can compensate the reduction of bearing capacity of footings.

Practically the two studies are based on software program, which provided a limited idea about the actual behavior of strip footing. This is due to the following points:

1- The analysis of the footing -soil-cavity interaction problem by using software program which does not take into consideration the effects of geogrid placed on state of soil.

2- The soil materials behavior were assumed to be governed by a linear or non linear elastic-plastic constitutive model based on one of theory failure criterion.

3- Numerical integration is used in the analysis of the strip footing because of difficulty or impossibility of direct integration in software program.

4- For program, the measured values of the strip settlement do not take into consideration the effects of waiting time between any two load increments during the model testing.

5- In software program, the behavior of the strip footing do not take into consideration the effects of the interface layer between geogrid and soil.

The main objective of this research is to reduce the risk of cavity development within sandy soil by using geogrid reinforced improvement technique. Also, to determine the combined effect of the width of the geogrid layer to diameter of cavity (b/d) with the following parameters: [Lateral location of the cavity (X/d), the depth of the first geogrid layer (h/d), the vertical distance between geogrid layers (S/d), and number of the geogrid layers (N)] on the bearing capacity ratio (BCR) of strip footing located on sandy soil with cavity when this soil reinforced with geogrid layers. Generally, this research presents the effect of several parameters on the strip footing stability where all these factors were not studied in the previous works.

## 3-Properties of geogrid layers

Geogrid, is defined as a geosynthetic formed by a regular network of integrally connected elements and possess apertures greater than 6.35 mm (1⁄4 inch) to allow interlocking with surrounding soil, rock, earth, and other surrounding materials to primarily function as reinforcement. Rib for geogrids is the continuous elements of a geogrid which are either in the machine (MD) or cross-machine direction (XMD) as manufactured, Junction is the point where geogrid ribs are interconnected to provide structure and dimensional stability. **(ASTM D6637-01-2009)**

Geogrid is stiff or flexible polymer grid-like sheets with large apertures used primarily for stabilization and reinforcement of unstable or week soil. The general types of geogrid are: Unidirectional geogrid, Bidirectional geogrid, Extruded geogrid, Bonded geogrid, and Woven geogrid. [**(ASTM D6637-01-2009) and Roberrt, 2005**].

The strength of the geogrids varies between20 and 250 kN/m, and they are used in both road constructions and reinforced slopes. Geogrids can be divided into two groups : Stiff geogrids, mostly high density polyethylene (HDPE) with a monolithic mesh structure. Flexible geogrids, mostly polyethylene terephthalate (PET) with poly vinyl chloride (PVC) or acrylic coating with mechanically connected longitudinal and transverse elements. [**Voskamp, 2003]**

The geogrid Tensar SS2 have tensile strength and elastic modulus higher than other geogrids made by different manufactures such as Netlon CE121, Iraqi geogrid, China geogrid, PMP SQ12, PMP SQ15, and PMP CE131. **[Al-Omari and Fekheraldin, 2012]**. Therefore the geogrid used in this research was geogrid Tensar SS2. It was manufactured by the British Company Netlon ltd. Many of the physical properties of geogrids including the weight (mass), type of structure, rib dimensions, junction type, aperture size, and thickness can be measured directly and are relatively straightforward as shown in Table (1). The mechanical properties of this type of geogrid are summarized in Table 2.

**Table 1: The physical properties of Tensar SS2 geogrids**

| Property | Unit | Data |
|---|---|---|
| Mesh Type | - | Square |
| Standard Color | - | Black |
| Polymer Type | - | **H**igh **D**ensity **P**oly**E**thylene, HDPE |
| Packing (Length/ Width) | m | Rolls (50/4) |
| Aperture Size (MD/XMD) | mm | 28/40 |
| Mass per Unit Area | $Kg/m^2$ | 0.3 |
| Rib Thickness | mm | 1.2/1.1 |
| Junction Thickness | mm | 3.9 |
| Longitudinal Rib Width | mm | 3 |
| Transverse Rib Width | mm | 3 |

**Table 2: The mechanical properties of Tensar SS2 geogrids After [Al-Omari and Fekheraldin, 2012]**

| Property | Unit | Data |
|---|---|---|
| Peak Tensile Strength MD/XMD | kN/m | 14.4/28.2 |
| Elastic Modules MD/XMD | GPa | 0.57/0.99 |
| Upper Yield Strength MD/XMD | MPa | 1/3 |
| Lower Yield Strength MD/XMD | MPa | 1/3 |
| Tensile Strength MD/XMD | MPa | 24/30.7 |
| Fracture Percentage Elongation MD/XMD | % | -98/-98 |
| Percentage Elongation at Maximum Load MD/XMD | % | 3.5/2.9 |
| Total Percentage Elongation MD/XMD | % | 5/4.25 |

## 4-Properties of Sandy Soil

Disturbed sample of the soil was brought from Al-Najaf city. The geotechnical properties of the soil used in this work was based on the following tests: the mechanical analysis (Figure 1), Proctor compaction test ( Figure 2), direct shear test, consistency index, and specific gravity tests which it performed in the laboratory. The physical properties of the granular soil used were estimated as shown in Table(3). The various chemical tests conducted on soil sample used and it can be seen in Table (4).

**Table(3): Physical properties of the soil**

| Property | Unit | Data |
|---|---|---|
| Soil Type | - | SP |
| Coefficient of uniformity | - | 3.62 |
| Coefficient of curvature | - | 1.23 |
| Maximum dry density | $kN/m^3$ | 20.58 |
| Optimum moisture content | % | 9.6 |
| Cohesion | $kN/m^2$ | 32 |
| Angle of shearing resistance | deg | 37 |
| Plasticity Index | % | 5 |
| Specific Gravity | - | 2.68 |

**Table(4): Chemical properties of the soil**

| Property | Unit | Data |
|---|---|---|
| Gypsum Content | % | 23 |
| $SO_3$ | % | 11.5 |
| ORG | % | 1.2 |
| $CaCO_3$ | % | 0.25 |
| pH | % | 7.9 |
| Cl | % | 0.18 |

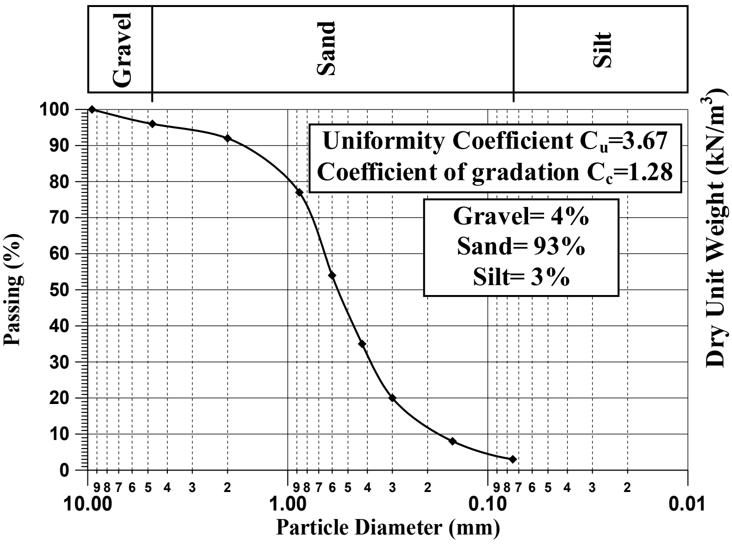


Figure(1): Grain size distribution curve for tested sample

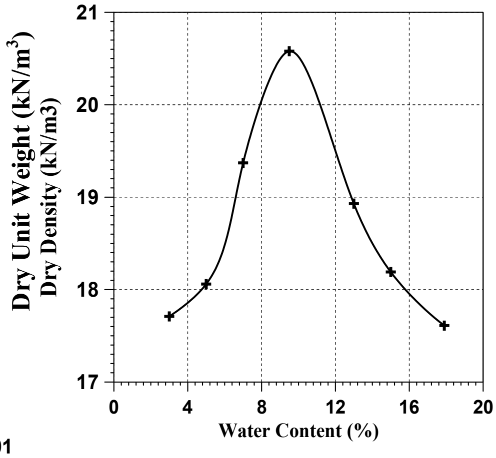


Figure(2): Compaction curve of soil sample

## 5-Testing Program

In order to investigate the bearing capacity of strip footing on sandy soil with cavity, forty five model tests were performed in laboratory. The dimensions of the strip model steel footing were breadth = 100 mm and length= 250 mm as shown in Figure(3). The bottom of the model footing was made rough by coating it with glue and then rolling it over sand. The bed of soil is prepared in the form of layers of 50 mm thickness. Water corresponding to optimum content was then added gradually and mixing with dry soil, care is taken to distribute the moisture evenly. The wet soil is compacted (to 95 % of maximum dry density) inside the container (Width=250 mm, Length=1250 mm, and Height=800 mm) using a flat bottomed steel block.

PVC pipe, 100 mm diameter was used to simulate the cavities. It was placed in required place during compaction process. Compaction continues until the final bed is achieved. After the completion of the bed of soil, the front side of steel box (soil container) as in Figure (4) is opened and the PVC tube is withdraw out of container slowly and the front side is placed again in its original position

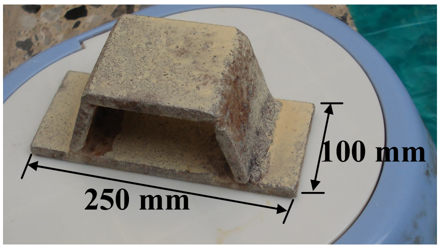


Figure(3): Strip footing apparatus

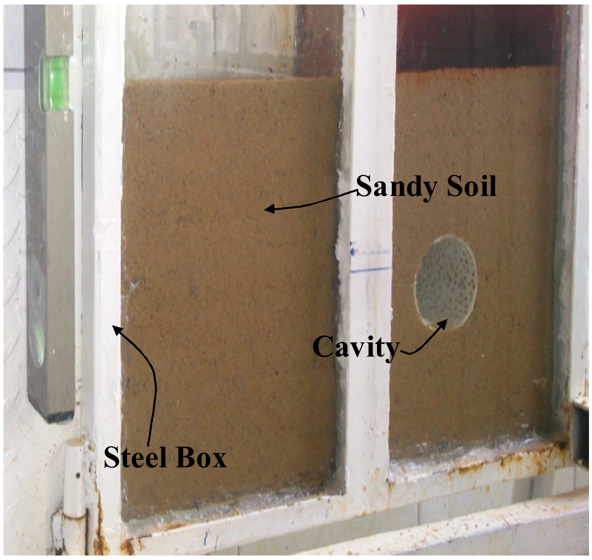


Figure(4): Preparation of the model test

The geogrid layers were placed in the sand at the desired position (h/d) and width (b/d) as shown in Figure(5), then strain gauges were fixed on the geogrid layer to recorded the developed strains at any applied loading by using strain gauge amplifier, data acquisition system, and laptop computer as shown in Figure (6). Many channels of automatic data were monitored at prescribed intervals starting at the beginning of construction using acquisition unit. The acquisition system has been designed and created to satisfy the requirements of all laboratories. Data collection takes place completely automatically. The data were transferred to a personal computer in which a windows based program with menu driven command selection is straightforward. Amplifier strain gauge is used to measure the reinforcement strains. It was defined as a circuit provides bridge voltage excitation and strain (ΔR) sensing on a single compact board. The circuit is powered by +5 V only. It was designed to be used with a 120 Ω full bridge.

The footing model was placed on the ground surface level ($D_f$=0). Two dial gauges were fixed on front and rear of strip footing which measure the average settlement. The dial gauges having a sensitivity of 0.01 mm accuracy. The initial readings of the dial gauges are recorded prior to any loading, then the vertical loads were applied incrementally to the strip footing through Universal Machine (an electrically operated hydraulic jack) and the corresponding settlements of the strip footing were recorded. The applied pressure at a constant increments of (50 kPa) (Stress Control Test).

The description of the parameters used to study the behavior of strip footing over reinforced soil with cavity were presented in Figure(7).

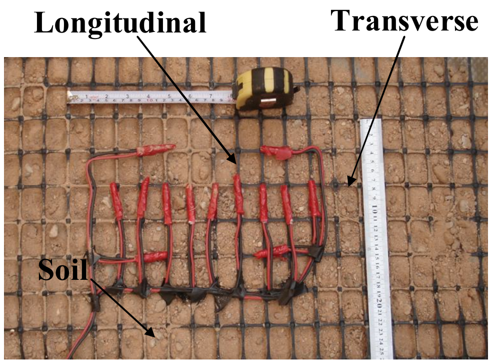

Figure(5): Placed of geogrid layer

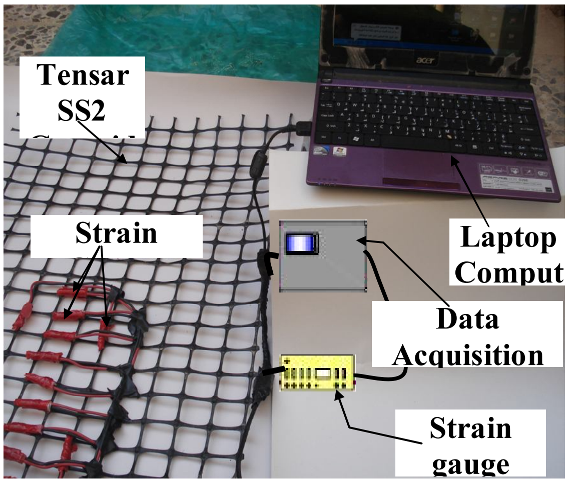

Figure(6): Strain gauges setup

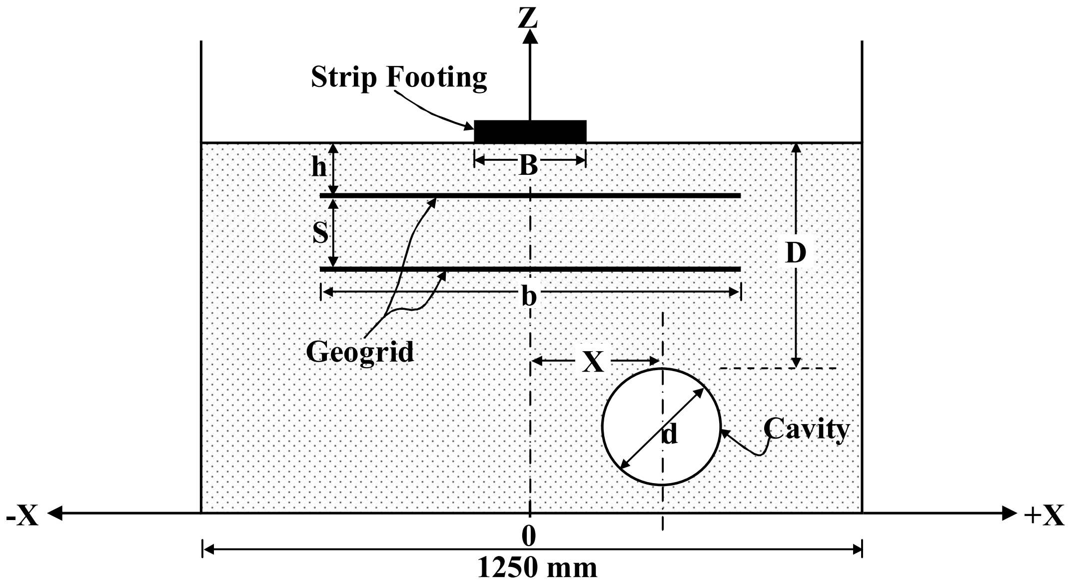

Figure(7): Schematic of strip footing-Soil-Cavity

## 6- Validity of Laboratory Work

No previous results for sandy soil reinforced with geogrid layer with the presence of cavities under application of vertical pressure testing are available, it is not possible to compare the experimental results herein directly with available literature.

The laboratory model tests of the present work has been validated by comparing some of the present results **(for no cavity case)** with that published by other workers **(for sandy soil without cavity)** such as Patra et al.(2005), and Shin and Das(2000). The results of the present work are plotted in the relationship between the applied stresses and corresponding settlement to compare them with Patra et al. (2005) results as shown in Figure(8). It is clear from Figure(8) that the deviation between the results is very small.

Figure(9) illustrates the results of the present work in term of bearing capacity ratio ( bearing capacity of the strip footing on reinforced to unreinforced soil by using four geogrid layers) versus the location of the first layer of geogrid (h/B) compared with previous work of Shin and Das (2000). The results of the present work are conservative as compared to Shin and Das (2000). Figure(10) shows the results of (BCR) versus the width of geogrid layers (b/B), where again the present work exhibited conservative results as compared to the previous published data.

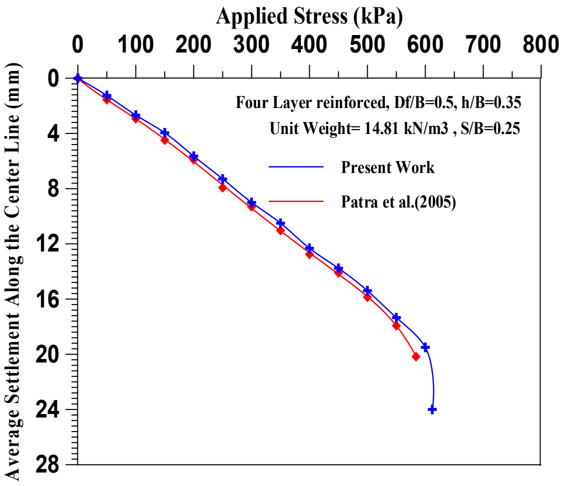


Figure(8): Comparison between the behavior of strip footing of present study and Patra et.al. (2005) for sandy **without cavity** .

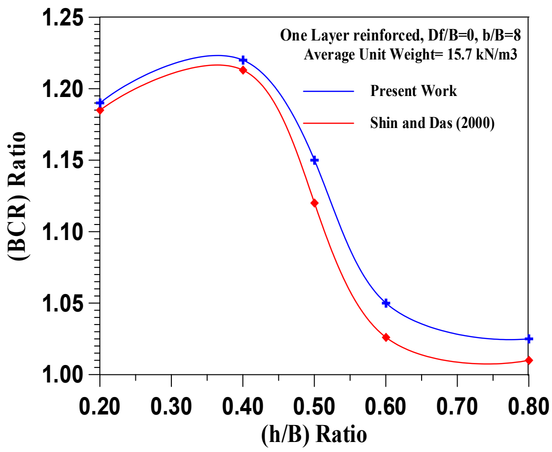


Figure(9): Comparison between the relationship between (BCR) ratio and (h/B) ratio of present work and Shin and Das (2000) for **no cavity condition**.

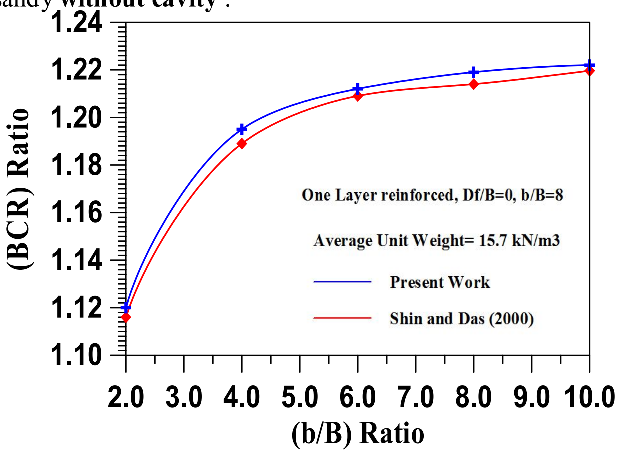


Figure(10): Comparison between the relationship between (BCR) ratio and (b/B) ratio of present work and Shin and Das (2000) for **no cavity condition**.

## 7-Results Discussion

To facilitate comparisons between the model tests, the geometric parameters are presented in terms of the dimensionless forms by dividing all parameters used in this work to cavity diameter (d). The model tests series involves Forty Five tests on model of strip footing with depth $D_f/d$=0 and width (B/d=1) . It is located on the compacted sandy soil with density corresponding to 95% of maximum dry density. The values of the diameter and depth of the cavity for all model tests are (d=100 mm) and (D=400 mm) respectively.

In the following sections, the combined effects of the presence of the cavity and the geogrid layers on the behavior of the strip footing are discussed.

In all model tests of this present work, the behavior of the initial portion of the applied pressure – settlement curves are linear. It becomes nonlinear behavior with increasing the applied pressure.

**(7-1) Combined effect of the cavity location and geogrid width on behavior of strip footing**

At a constant depth of one geogrid layer (h/d=2), sixteen model tests were conducted on reinforced and unreinforced soil.

Figure(11a) shows applied stress – average settlement curves for different values of the lateral cavity position (X/d) ranging from (0 to 3) for unreinforced soil (without geogrid layer at zero width of geogrid layer, b/d=0). It is obvious from this figure that the increase in the horizontal distance between footing and cavity (X/d) decreases the average settlement under strip footing. For example, at constant applied pressure of 600 kPa, the corresponding settlement ($\delta$/d) decreases from (0.32) for (X/d=0) to (0.253, 0.2 and 0.14) for (X/d= 1, 1.5 and 3 ) respectively. These results indicate that the differences between the curves depend on the distance ratios of the cavity (X/d).

When the soil is reinforced with low width of geogrid layer (b/d=1) and when the cavity is located at different position (ranging from X/d =0 to 3) , the pattern of the footing settlement is the same for the settlement of strip footing on unreinforced soil as demonstrated in the Figure(11b). This is due to that, the failure mechanism at the end of the model tests for unreinforced or reinforced soil with small width of geogrid layer is observed as a punching of the strip footing into the sandy soil with cavity ( the top of soil block wedge represent the base of strip footing, but the bottom of soil block wedge represent the cavity crest).

The increase in the width of the geogrid layer is very effective in increasing the bearing capacity and decreasing the settlement. By inspection of Figure(11c), it can be noticed that the values of the footing settlement for model test with cavity position (X/d=3) are smaller than those for model tests with cavity (X/d= 0), but the values of settlement of model test (X/d=1 and 1.5) are greater than those the cavity placed at position under the centerline of the strip footing (X/d=0). This due to that the geogrid layer will prevent the movements of the soil particles toward cavity. At working carrying stress of (600 kPa), the corresponding values of the settlement of the strip footing from Figure(11c) are ($\delta$/d= 0.12, 0.139, 0.17 and 0.18) for (X/d=3, 0, 1.5 and 1 ) respectively.

The behavior of strip footing is reversed with the increasing of the width of geogrid layer to (b/d=7.5) as shown in Figure(11d). The figure demonstrates that the values of the settlement are decreased with decreasing the lateral distance between centerline of cavity and strip footing. This family of curves remained in agreement with themselves. In other means, for high value of (b/d) ratio the changing of the value of the cavity location has only a slight influence on the characteristic of the stress – settlement curve, but for the cases with low geogrid width, the cavity position (X/d) has a great effect on the strip footing behavior.

The results of the case of cavity with (X/d=3) are much close together although the settlements of the strip footing of the geogrid length with (b/d=0) and (b/d=1) record the highest values at any load increments.

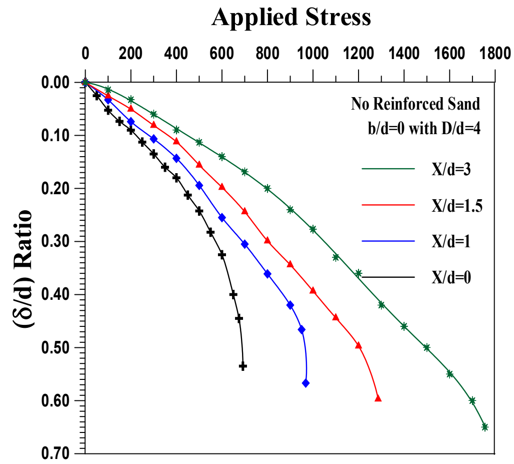


Figure(a):Variation of applied stress with average vertical settlement of footing for no reinforced case.

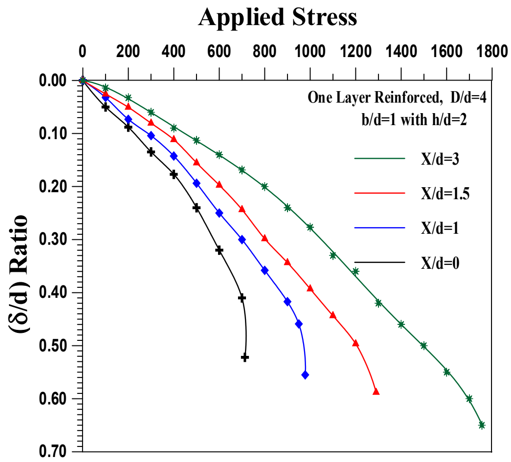


Figure(b):Variation of applied stress with average vertical settlement of footing for reinforced case (b/d=1)

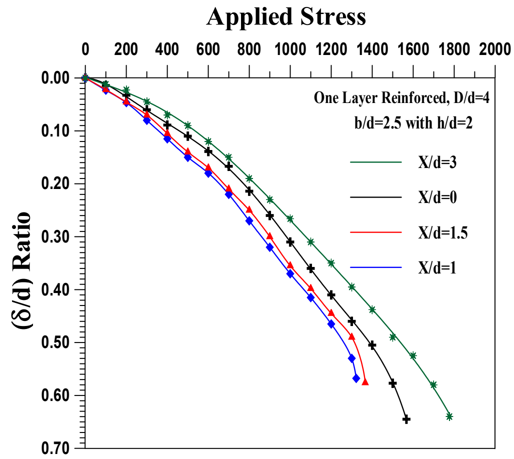


Figure(c):Variation of applied stress with average vertical settlement of footing for reinforced case (b/d=2.5)

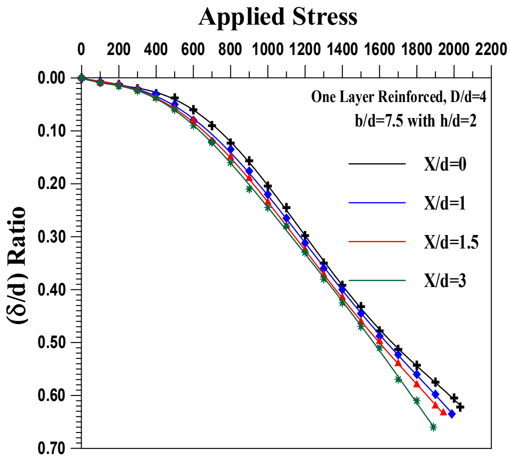


Figure(d):Variation of applied stress with average vertical settlement of footing for reinforced case (b/d=7.5)

Figure(11): Results of model tests for depth ratio (h/d=2) and (D/d=4) at different values of (X/d) ratio for reinforced and unreinforced soil

### (7-2) Combined effect of the depth and width of the geogrid layer on the behavior of strip footing

From the previous section can be noted that the effect of the cavity is more critical when the location of the cavity is (X/d=0). Therefore in this category, the model tests are performed on soil with cavity location (X/d=0). At a diameter of the cavity is equal to the width of the geogrid layer (b/d=1), the higher generated settlement under the strip footing is noted when the geogrid layer is located at high depth (h/d=3) for the same applied stress as shown in Figure (12a). At working applied stress of (500 kPa), the corresponding values of the settlement of the strip footing (δ/d) are (0.13, 0.186, 0.24 and 0.28) for depth ratio (h/d= 0.5, 1, 2, and 3) respectively.

When the width of the geogrid is increased to (b/d=2.5), the behavior of the strip footing is changed in which the load-displacement curve of model test with (h/d=2) gives highest resistance as shown in Figure(12b).The values of the footing settlement of the model tests with (h/d ≤1)are greater than the settlements of model tests with(h/d=2 and 3).

Figure(12c) depicts the variation of footing settlement with applied stress at geogrid width (b/d=7.5). In this plot, the settlement of the footing are very small when the geogrid layer depth is very high ( the geogrid layer is very near from the crest of the cavity) condition (h/d=3). This is probably due to the fact that the presence of the geogrid layer will lead to that the cavity is not located in the influence zone of the strip footing loaded. With the increase in the (h/d) values, the soil resistance increased for high width of the geogrid, opposite behavior can be noted when the soil is reinforced with low width of geogrid layer. This behavior may be due to the width of the geogrid layer is equal to the diameter of the cavity. This is because the movements of the soil particles in vertical direction towards the cavity becomes greater than the movements in horizontal direction.

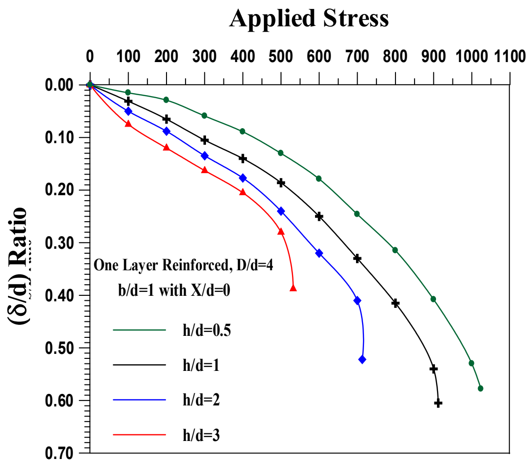


Figure(a):Applied stress versus settlement of footing for reinforced case with geogrid length (b/d=1).

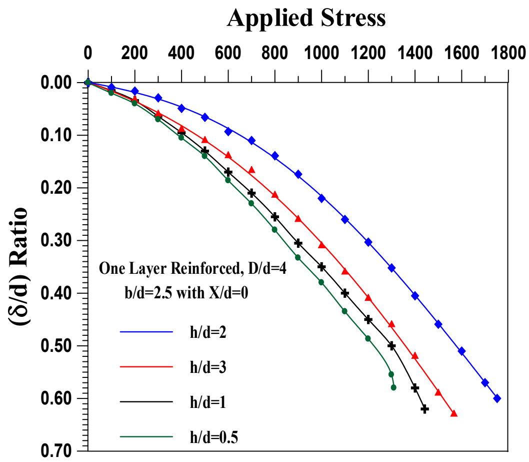


Figure(b):Applied stress versus settlement of footing for reinforced case with geogrid length (b/d=2.5).

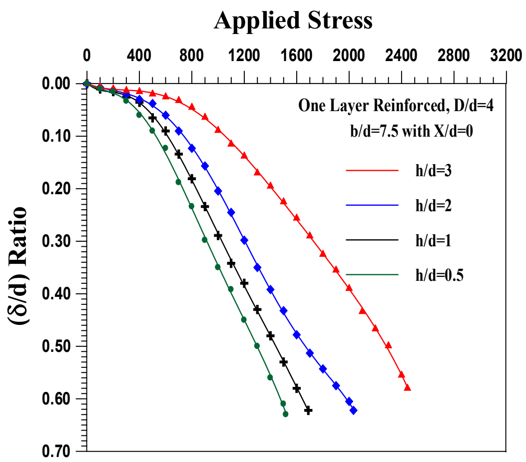


Figure(c):Applied stress versus settlement of footing for reinforced case with geogrid

Figure(12): Results of model tests for cavity position (X/d=0) and (D/d=4) at various values of depth ratio (h/d) and width ratio (b/d) of the geogrid layer

### (7-3) Combined effect of the vertical distance between geogrid layers and geogrid width on the behavior of strip footing

In this section, the model tests are conducted at lateral location of the cavity (X/d=0), its location is more danger on the footing stability than other locations. Figure(13a) illustrate the behavior of strip footing on soil reinforced with two layers of geogrid, which the load-displacement curve of model test with (S/d=0.5) is very much closer with the model test (S/d=1) when the width of the geogrid layer is small (b/d=1). This behavior of the strip footing happened due to the collapse of footing – soil- geogrid system occurred as a block wedge form. The settlement values of both previous cases are smaller than those for two cases (S/d=1.5 and 3).

The results of the settlement of footing on soil reinforced with geogrid layer (b/d=2.5) are presented in Figure (13b), from which it can be seen that, at any increments, the values of the footing resistance for model test with distance ratio (S/d=1.5) are higher than those for model test with distance ratio (S/d=3). Opposite behavior can be noted at high geogrid width (b/d=7.5) as shown in Figure (14c).The Figure(13c) demonstrate the relationship between the applied stress with the development of the settlement when the soil with geogrid (b/d=7.5). Based on the results of the figure, for three cases (S/d=0.5, 1.5, and 3), the curves remained in agreement with themselves up to applied stress of (700 kPa). After this stress, the differences between the curves are approximately equally.

In general, the effect of the presence of the geogrids layers at distance ratio (S/d=1) is much more significant in the increase of the footing resistance at any value of the width of the geogrid specially when (b/d) is greater than (2.5) (the optimum value of (S/d) ratio is one). When the width ratio (b/d >1), the lowest resistance of the strip footing can be observed at (S/d=0.5).

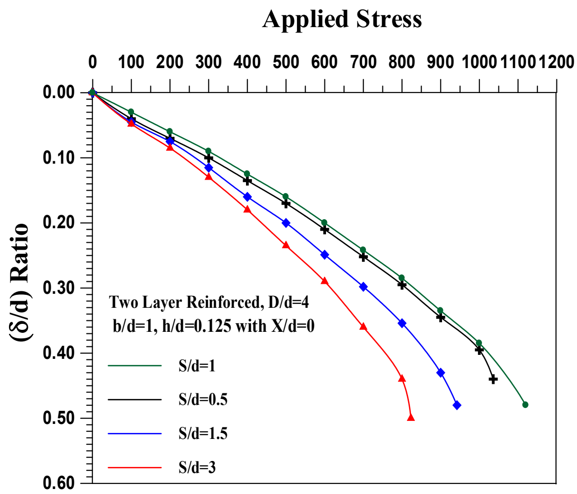


Figure(a):Applied stress – footing settlement curve for two layer reinforced with geogrid length (b/d=1).

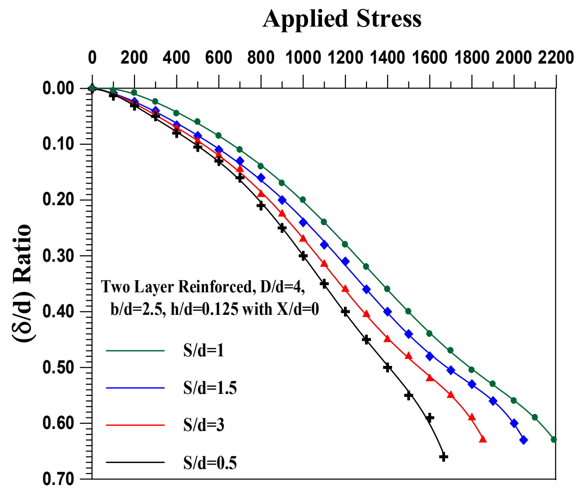


Figure(b):Applied stress – footing settlement curve for two layer reinforced with geogrid length (b/d=2.5).

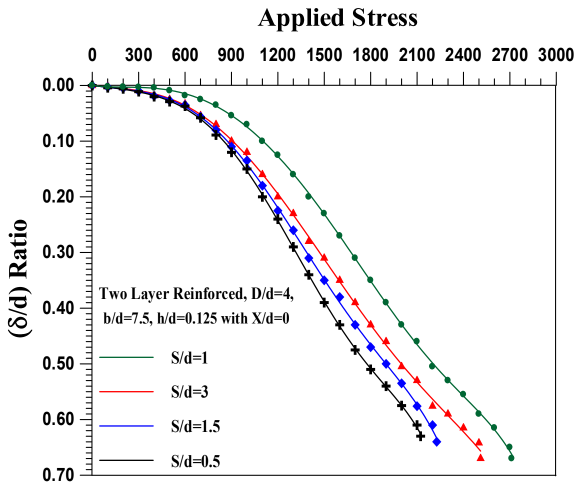


Figure(c):Applied stress – footing settlement curve for two layer reinforced with geogrid length

Figure(13): Results of model tests for cavity position (X/d=0), (h/d=0.125) and (D/d=4) at various values of vertical distance between two layer of geogrid (S/d) ratio and (b/d) ratio

### (7-4) Combined effect of number of geogrid layers and geogrid width on the behavior of strip footing

To study the effect to increase number of reinforced layer, nine model tests were conducted when the cavity position is located under centerline of strip footing (X/d=0), the vertical distance between any two geogrids is (optimum value of S/d=1) and at various values of width of geogrid layers (b/d) as shown in Figure(14).The family of the applied stress – footing settlement curves are presented in Figure (14a). It can be noted from this Figure that the settlement of footing increases due to the increase in number of the geogrid layers at any applied stress increment. This behavior of strip footing is due to that the width of the geogrid used into soil is small (b/d=1).

Figure (14 b) demonstrates the applied stress –settlement curves for model tests with (b/d=2.5). As indicated by the figure, despite the number of layer (N=3) is lower than (N=4), the resistance for model test with (N=3) is greater than that the resistance for model with four geogrid layers. The three curves for all model tests are coincided together up to stress of (300 kPa).

Figure (14c) is similar to those for relations between the applied stress and the corresponding settlement in Figure(14b), but the curves in Figure (14c) coincided up to stress of (900 kPa). Beyond this stress, the strip footing on soil with number of geogrid layer (N=3) carries more applied stress than the footing on soil with number of geogrid layer (N=4) and (N=2) respectively.

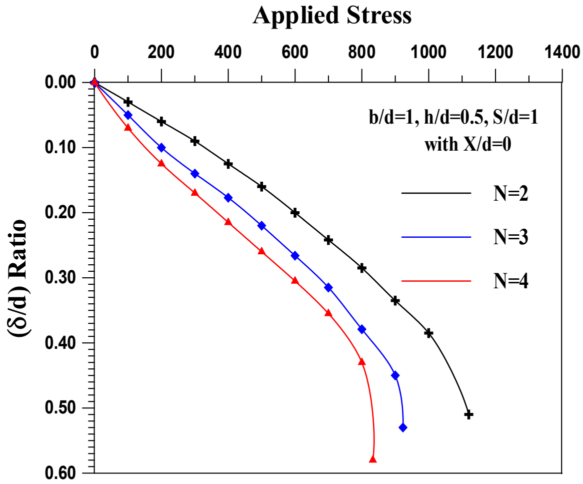


Figure(a):Relationship between applied stress and (δ/d) for reinforced case with geogrid length (b/d=1).

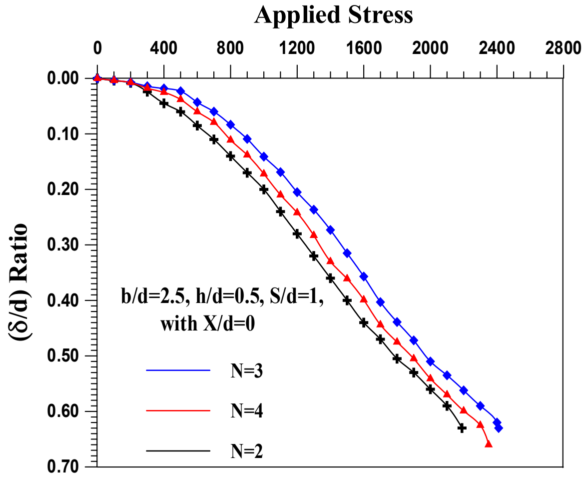


Figure(b):Relationship between applied stress and (δ/d) for reinforced case with geogrid length (b/d=2.5).

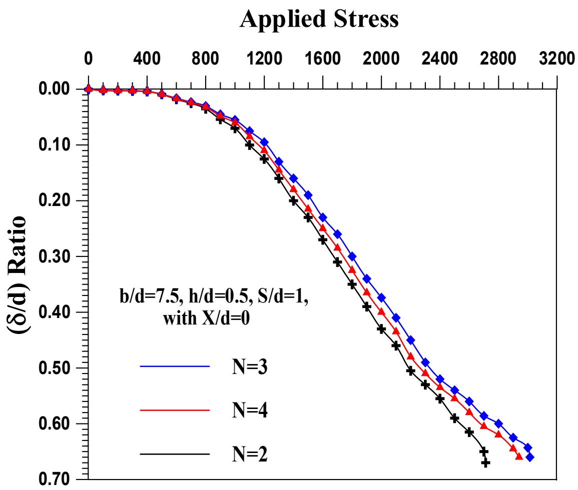


Figure(c):Relationship between applied stress and (δ/d) for reinforced case with geogrid length (b/d=7.5).

Figure(14): Results of model tests for cavity position (X/d=0), (h/d=0.5), (S/d=1) and (D/d=4) at various values of number of geogrid layers and (b/d) ratio

To compare between the behavior of strip footing on sandy soil with and without cavity can be noted that for sandy soil without cavity and reinforced with number of the geogrid layers, Al-Omari (1995) concluded that there may be limiting reinforcement stiffness, influenced by the number of reinforcing layers after which there will be no further gain in strength. But for sandy soil with cavity and reinforced with number of the geogrid layers, from the present work can be concluded that the optimum value of the number of geogrid layers is three (N=3).

### (7-5) Bearing Capacity of Footing

The behavior of strip footing is analyzed in terms of its bearing capacity and the generated settlement. The values of the ultimate bearing capacity for different model tests has been estimated from the applied stress – settlement curves. It is observed that the failure applied stress is the point at which the slope of the curve becomes constant at minimum value. In other words, the failure applied stress can be estimated at which the curve exhibits a peak or maintains continuous settlement increase with no further increase in applied stress.(Patra, 2005).

To facilitate comparisons between the model tests, the values of the bearing capacities are presented in terms of the bearing capacity ratio (BCR). The bearing capacity ratio is defined as in equation(1).

$$BCR = \frac{q}{q_n} \qquad (1)$$

Where:

q = the ultimate bearing capacity of sandy soil with cavity when the soil is reinforced with geogrid.

$q_n$= the ultimate bearing capacity of sandy soil with cavity when the soil is not reinforced with geogrid.

Relationships among cavity location ratios (X/d), geogrid width (b/d) and bearing capacity ratio (BCR) are shown in Figure( 15 ). It is obvious from this figure that the bearing capacity ratios of the strip footing linearity increases as the width of the geogrid layer increases when the cavity is located at horizontal distance (X/d=1, 1.5 and 3). The shape of the (BCR) ratio - (b/d) ratio curve of the case (X/d=0) is non – linear. This is probably due to the fact that the presence of the geogrid layer of the case (X/d=0) lead to the rate of pushing of the soil particles toward the cavity is slower than that for the other cavity positions (X/d=1, 1.5 and 3). When the cavity is located at high ratio (X/d=3), the curve for this condition is almost horizontal (slight effect of width of geogrid layer) and the vertical distance between other curves are increased with decreasing the value of (X/d) ratio.

Figure (16) shows the variations of the bearing capacity ratio with the width and depth of the geogrid layers. It is seen from the figure, that when the width of the geogrid layer was high (b/d), the maximum increase in bearing capacity ratio occurred at high depth of geogrid layer (h/d=3), but this behavior is inversed with decreasing the width ratio. In other words, at width ratio (b/d=1) and depth ratio (h/d=3), the value of the bearing capacity of reinforced soil is smaller than those of the unreinforced soil (BCR<1). Generally, the effect of the width of the geogrid on the resistance of the strip footing increases with the increase of geogrid depth to (h/d= 2 and 3). Also, when the geogrid layers are near the ground surface level (h/d=0.5 and 1), the increase in values of BCR ratio are small with increasing the width of geogrid layer (the width of the geogrid layer has only a slight influence on the characteristic of the strip footing resistance). The two curves of these cases are flat.

When the soil is reinforced with two layers of geogrid, the bearing capacity ratio (BCR) are plotted against the width of the geogrid layer (b/d) at various values of the vertical distance between the geogrid layers (S/d) as shown in Figure (17). The figure show that the BCR increases with increasing the width of the geogrid layer at any value of (S/d). Also, the figure demonstrates the rate of the increase in bearing capacity ratio (BCR) is very high with the increase in the width of the geogrid when the value of (S/d=1). The lowest values of footing resistance can be observed at vertical distance between the geogrid layers (S/d=0.5). It can be noted that when the width of the geogrid layer is high (b/d=7.5), the strip footing on soil with (S/d=3) reaches to its resistance first followed by the strip footing on soil with (S/d=1.5 and 0.5) respectively.

The results of the bearing capacity ratios of the number of geogrid layers (N=3 and 4) conditions are much close together although the case of geogrid (N=3) record the highest values of the bearing capacity ratio at geogrid width (b/d >1) as shown in Figure(18). Also, it can be illustrated from this figure that the higher number of geogrid layer (N=4) with lower width of the geogrid layer (b/d=1) has a lower bearing capacity ratio. This is because the faster movement of the failure soil block (high weight of the soil – geogrid system) in vertical direction to wards the cavity. The effects of number of layers (N=2) on the bearing capacity ratio of strip footing are small at high values of geogrid width.

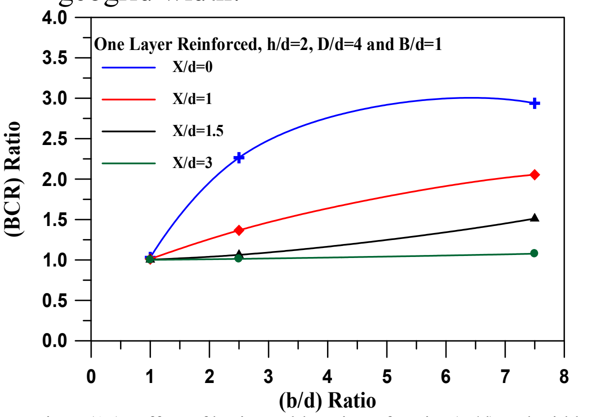


Figure(15): Effect of horizontal location of cavity (X/d) and width of geogrid (b/d) on BCR ratio

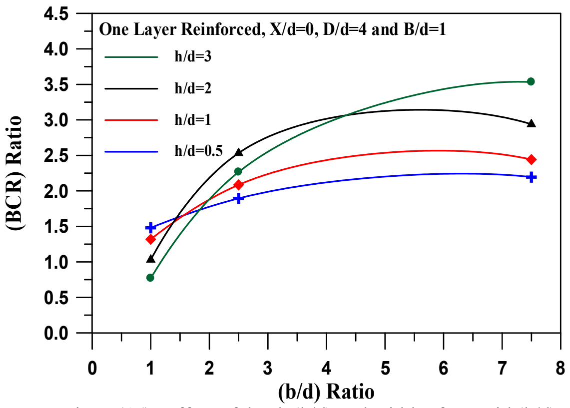


Figure(16): Effect of depth (h/d) and width of geogrid (b/d) on BCR ratio

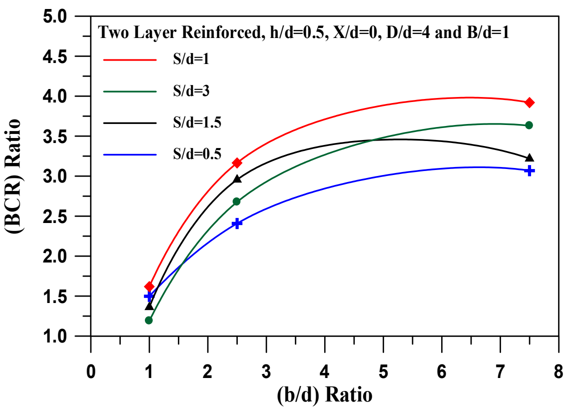


Figure(17): Effect of vertical distance between geogrid layers (S/d) and width of geogrid (b/d) on BCR ratio

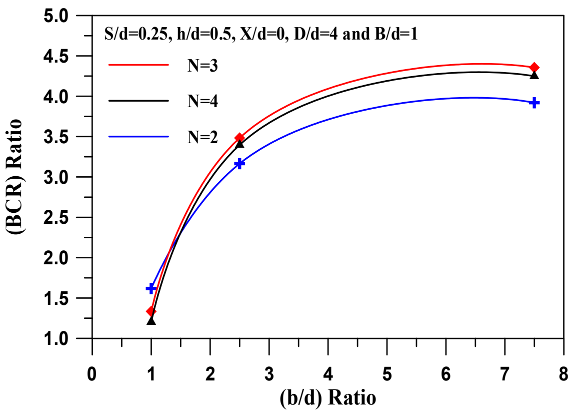


Figure(18): Effect of number of geogrid layers (N) and width of geogrid (b/d) on BCR ratio

**(7-6) Geogrid Strain Measurement**

Strain gauges were bonded directly to the surface of the geogrid reinforcement layers in this work. Strain gauges were concentrated in the top layer based on the expectation that the magnitude of reinforcement strains would be greater for layers closest to the base of the footing. However, the strain gauge readings did not provide quantitative data at incipient collapse for the soil. [Bathurst et. al (2003)].

In order to compare between different model tests, the reinforcement strains were observed at constant level of applied pressure of (1500 kPa). This is due to that the large strains were noted during applied stress increments between from 1500 kPa to failure.

The benefit of the determination of the strain values in geogrid layer to know the values of the development stress in geogrid layer depending upon modulus of elasticity as seen in equation (2). Thus lead to estimate the relationship between the behavior of the strip footing and geogrid layer.

$$\sigma = E * \varepsilon \qquad \text{.......(2)}$$

In general, the strain gauge readings (values of reinforcement strain) are reduced wherever the strain gauge located away from the strip footing in both horizontal directions (left and right directions of strip footing).

The strains in geogrid layer due to applied pressure of (1500 kPa) are plotted as a function of cavity location (X/d), at constant values of ratios (D/d=4), (h/d=2), (B/d=1) and geogrid width (b/d=7.5) as shown in Figure(19). It can be seen from the figure that the locations of peak strain gauge readings were consistent with the location of the cavity. The peak strain locations were (14.6, 14.6, 43.8, 43.8 and 73 mm) from the centerline of the strip footing for the no cavity condition and cavity locations (X/d=0, 1, 1.5 and 3) respectively. The recorded values of reinforcement strain increased with increasing horizontal distance between cavity and footing (X/d). Due to the presence of the cavity into soil at specific (X/d), the magnitudes of reinforcement strain in the right and left directions of strip footing are unequal as shown in Figure (19). When the cavity is located in the right direction of the strip footing, the values of the strain in this direction are greater than those in the left direction.

Figure (20) shows the distribution of development strain of the geogrid layer when the geogrid layers are located at different depth ratio (h/d). It is obvious from this figure that the magnitudes of reinforcement strains increases as the geogrid layers were near from the final bed of the soil surface level.(i.e h/d decreases). For any value of depth ratio (h/d) at applied pressure equal to (1500 kPa), the peak values of the strains can be observed at horizontal distance of (14.6 mm) or (-14.6 mm) from the centerline of the strip footing.

Figure(21) depicts the shapes of strain curves of model tests of the first geogrid layer at various vertical distance between these geogrid layers (S/d=0.5, 1, 1.5 and 3). It is clear that the lowest values of strain in geogrid layer when the distance between the geogrid layers (S/d=1), while it becomes maximum for (S/d=0.5) case at applied pressure of (1500 kPa).

Strain values of the first geogrid layer under applied stress of (1500 kPa) plots for three model tests different in number of geogrid layers (N=2, 3 and 4) are illustrated in Figure(22), which shows that the magnitudes of strains for three geogrid layers case (N=3) were smaller than that of the soil reinforced with two and four layers of geogrid

(N=2 and 4). This is due to the fact that the resistance of the strip footing soil against failure of model test (N=3) was greater than the model tests with (N=2 and 4).

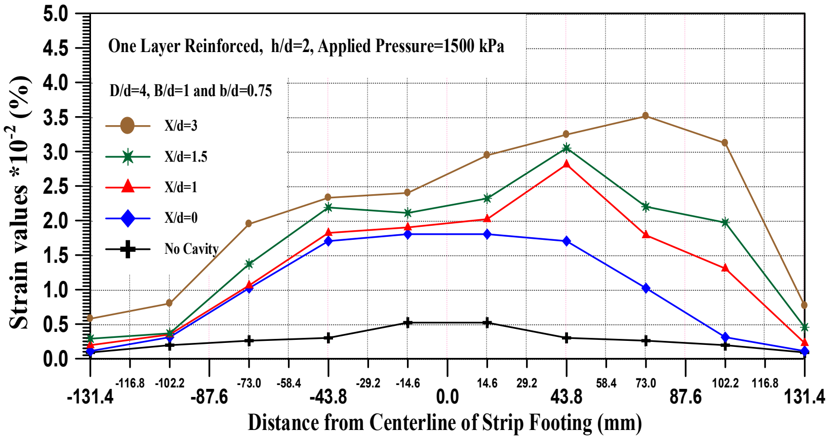


Figure(19): The reinforcement strains values at working stress of (1500 kPa) for the cases with and without cavity at various cavity position (X/d)

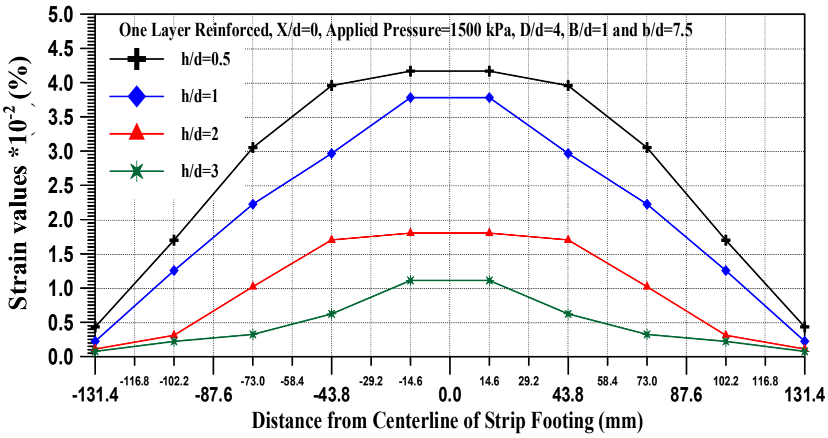


Figure(20): Results of reinforcement strains of model tests for different values of geogrid depth conditions (h/d) at applied stress of (1500 kPa)

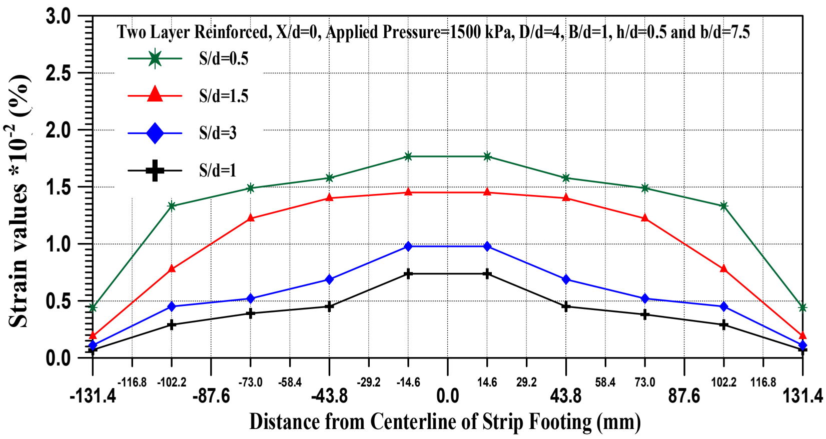


Figure(21): The development strains in first layer of geogrid of model tests for different values of the vertical distance between two geogrid layers

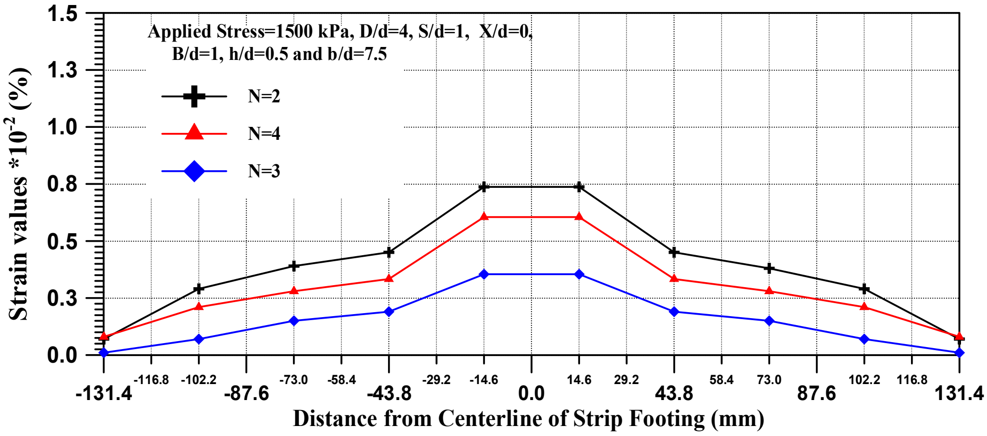


Figure(22): Effect of number of geogrid layers on the values of development strains in first layer of geogrid at applied stress of (1500 kPa)

## 8- Conclusions

Based on the results of the present work, the following conclusions can be drawn:

1- In general, the presence of the cavity within sandy soil without reinforcement reduces the effective shear strength and accelerates the development of the settlement of the strip footing, due to this the failure can occur faster and sudden failure (punching of the strip footing into the sandy soil with cavity) can takeplace.

2- For unreinforced sandy soil or reinforced soil with width of geogrid layer equal to the diameter of cavity (b/d=1) , the higher generated settlements of strip footing are noted when the cavity located at zero horizontal distance ratio (X/d) for the same applied stress. The increase in the width of the geogrid layer (b/d > 1) is very effective in increasing the bearing capacity and decreasing the settlement of strip footing.

3- For high value of reinforcement width (b/d ≥7.5) ratio, the changing of the value of the horizontal cavity location (X/d) has only a slight influence on the characteristic of the stress – settlement curve. For all of the cavity locations into soil (X/d) with reinforcement geogrid width (b/d=1) show results similar to those found in models with no reinforced soil (b/d=0) condition in values.

4- At any level of applied stress, the maximum settlement under strip footing occurred at a geogrid depth (h/d=3) for the case of small value of geogrid width (b/d ≤1). When the geogrid depth is located at mid vertical distance between the base of strip footing and the crest of the cavity, the load carrying capacity of the footing with (b/d=2.5) is higher than those for the cases with (h/d=0.5, 1 and 3 ). At high geogrid width (b/d=7.5), the rate of the generated footing settlement with applied stress is very high for the shallow geogrid and becomes low for deep geogrid.

5- The effect of the presence of two geogrids layers at distance ratio (optimum value of S/d=1) is much more significant in the increased of the footing resistance at any value of the width of the geogrid, specially when (b/d) is greater than (2.5), but at (S/d=0.5), the values of footing resistance are lowest.

6- For width of geogrid (b/d >1), the strip footing on soil with number of geogrid layer (N=3) carries more applied stress than the footing on soil with number of geogrid layer (N=2) and (N=4). In other words, the optimum value of number of geogrid layer is 3. The settlement of footing increases due to the increase in number of the geogrid layers when the width of the geogrid layer (b/d ≤1) at any applied stress increment.

7- The increase in bearing capacity ratio with width of geogrid layer are linear for the cavity located at (X/d=1, 1.5 and 3). The highest values of BCR are observed at cavity with (X/d=0) and the relation (BCR versus b/d) becomes non-linear.
8- The geogrid width has only a slight influence on the footing response, when the cavity is located at high ratio (X/d=3). In other words, the curve between (BCR versus b/d) for this condition have an approximately horizontal slope.
9- When the width of the geogrid layer was high (b/d), the maximum increase in bearing capacity ratio occurred at high depth geogrid layer (h/d=3). For soil reinforced with geogrid layer (b/d=1) and (h/d=3), the value of the bearing capacity of reinforced soil is smaller than those of the unreinforced soil (BCR<1).
10- The increase in values of BCR ratio are small with increasing the width of geogrid layer when the geogrid layers are near the ground surface level (h/d=0.5 and 1). The effect of the width of the geogrid on the (BCR) increases with the increase of geogrid depth to (h/d= 2 and 3).
11- Large strains of reinforcement were observed during applied pressures increments between from 1500 kPa to failure. The values of reinforcement strain are reduced wherever the strain gauge located away from the strip footing in both horizontal directions.
12- For all model tests, the magnitudes of reinforcement strain in the right and left directions of strip footing are unequal. The location of peak strain gauge readings is depend upon the cavity position (X/d). The magnitudes of the reinforcement strains in the right direction of footing are greater than the left direction when the cavity located in the right direction of footing.
13- The decrease in the distance between the centerline of the cavity and footing cause a decrease in reinforcement strains. As the geogrid layers were near from the base of strip footing, the values of reinforcement strains increased.
14- The magnitudes of strains for three geogrid layers (N=3) were smaller than that of the soil reinforced with two and four layers of geogrid (N=2 and 4).

**<u>9- References</u>**

Al-Fares, R.A.(2008), ***"Cavities Detection and Treatment at a Residential Area Under Development in the state of Kuwait"*** Sinkholes and the Engineering and Environmental Impacts of Karst, 2008.

Al-Omari, R.R., Nazhat, Y.N. and AL-Dobaissi, H.H. (1995) ***"Effect of Stiffness and Amount of Reinforcement on Strength of Sand"*** Journal of Engineering Geology, pp. 363-367.

Al-Omari, R. R. and Fekheraldin, M. K. (2012), ***" Measurement of Tensile Properties of Geogrid"***, Second International Conference on Geotechnique, Construction Materials and Environment, Kuala Lumpur, Malaysia, Nov. 19-21, ISBN: 978-4-9905958-1-4.

Al-Sinaidi, A., R. and Ali, A. H. (2006), ***" Improvement in Bearing Capacity of Soil by Geogrid – an Experimental Approach"***, IAEG Journal, No.240

ASTM D6637-01-2009, (2009) ***"Standard Test Method for Determining Tensile Properties of Geogrids by the Single or Multi-Rib Tensile Method"***.

Bathurst, R. J., Blatz, J. A. and Burger, M. H. (2003), ***"Performance of instrumented large-scale unreinforced and reinforced embankments loaded by a strip footing to failure"***, Canada Geotechnical Journal, Volume 40, PP. 1067–1083.

Gabr, M. A. and Hunter, T. J. (1994), "***Stress-strain analysis of geogrid-supported liners over subsurface cavities",*** Geotechnical and Geological Engineering, June, Volume 12, Issue 2, PP 65-86.

Ghazavi, M. and Soltanpour, Y. (2008), "***Effect of Cavity on Bearing Capacity of Shallow Foundations in Geotextile-Reinforced Soil",*** The 12th International Conference of International Association for Computer Methods and Advances in Geomechanics (IACMAG), 1-6 October, Goa, India.

Omar, M.T., Das, B.M., Puri, V.K., Yen, S.C. and Cook, E.E. 1993***."Ultimate bearing capacity of rectangular foundations on geogrid reinforced sand"***, Geotechnical Testing Journal, ASTM, Volume 16, Issue 2, PP.246-252.

Patra, C.R., Das, B.M., and Shin, E. C. (2005), ***"Ultimate Bearing Capacity of Eccentricity Loaded Strip Foundation on Sand Reinforced with geogrids"***, International Symposium on Tsunami Reconstruction with Geosynthetics, 8 to 9 December 2005, Bangkok.

Roberrt M. Koerner, (2005), ***Designing with Geosynthetics***, Library of Congress Cataloging: Publisher's, Chapter 3.

Shin, E.C. and Das, B.M.(2000), " Experimental Study of Bearing Capacity of a Strip Foundation on Geogrid – Reinforced Sand", Geosynthetics International, Volume 7, No.1, PP. 59-71.

Voskamp W. (2003) ***" Performance Properties of Geogrids"*** Reinforced Soil Engineering. Advances in Research and Practice, 4th ed. vol. 1, Hoe I. Ling, Dov Leshchinsky and Fumio Tatsuoka, Ed. Library of Congress Cataloging: Publisher's, pp. 32-48.